BIOCHEMISTRY
including biophysical chemistry & molecular biology

Article

pubs.acs.org/biochemistry

Kinetic and Thermodynamic Rationale for Suberoylanilide Hydroxamic Acid Being a Preferential Human Histone Deacetylase 8 Inhibitor As Compared to the Structurally Similar Ligand, Trichostatin A

Raushan K. Singh,*[,†] Naveena Lall,[†] Travis S. Leedahl,[†] Abigail McGillivray,[†] Tanmay Mandal,[†] Manas Haldar,[‡] Sanku Mallik,[‡] Gregory Cook,[†] and D. K. Srivastava*[,†]

[†]Department of Chemistry and Biochemistry, North Dakota State University, Fargo, North Dakota 58102, United States

[‡]Department of Pharmaceutical Sciences, North Dakota State University, Fargo, North Dakota 58102, United States

ABSTRACT: Of the different hydroxamate-based histone deacetylase (HDAC) inhibitors, suberoylanilide hydroxamic acid (SAHA) has been approved by the Food and Drug Administration for the treatment of T-cell lymphoma. Interestingly, a structurally similar inhibitor, trichostatin A (TSA), which has a higher *in vitro* inhibitory potency against HDAC8, reportedly shows poor efficacy in clinical settings. To gain molecular insight into this discriminatory feature, we performed transient kinetic and isothermal titration calorimetric studies for the interaction of SAHA and TSA with the recombinant form of human HDAC8. The transient kinetic data revealed that the binding of both inhibitors to the enzyme showed biphasic profiles, which represented an initial encounter of the enzyme with the inhibitor followed by the isomerization of the transient enzyme−inhibitor complexes. The temperature-dependent transient kinetic studies with these inhibitors revealed that the bimolecular process is primarily dominated by favorable enthalpic changes, as opposed to the isomerization step, which is solely contributed by entropic changes. The standard binding enthalpy ($\Delta H°$) of SAHA, deduced from the transient kinetic as well as the isothermal titration calorimetric experiments, was 2−3 kcal/mol higher than that of TSA. The experimental data presented herein suggest that SAHA serves as a preferential (target-specific and -selective) HDAC8 inhibitor as compared to TSA. Arguments that the detailed kinetic and thermodynamic studies may guide the rational design of HDAC inhibitors as therapeutic agents are presented.

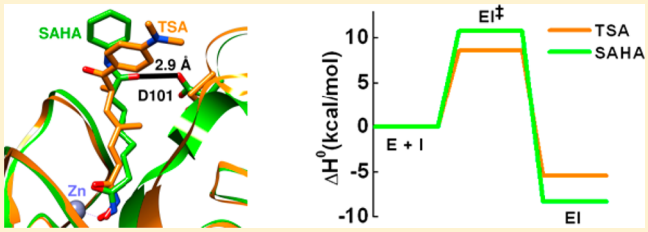

The acetylation and deacetylation of a specific lysine residue of the histone tail mediated via histone acetyl transferase (HAT) and histone deacetylase (HDAC), respectively, play a pivotal role in eukaryotic gene expression.[1] Aside from histones, more than 3700 distinct lysine acetylation sites have been identified in the human proteome, which serve as targets for the enzymes described above.[2] Various cellular processes such as cell growth and differentiation, DNA replication and recombination, metabolism, cell signaling, etc., are regulated via the acetylation and deacetylation of myriad varieties of non-histone proteins.[3] Because HDACs cause deacetylation of acetylated lysine moieties present on a wide variety of non-histone proteins, these enzymes should appropriately be called "lysine deacetylases".[2]

Human HDACs have been classified into four groups based on the homology of their gene sequence. Class I (HDAC1, -2, -3, and -8) and class II (HDAC4, -5, -6, -7, -9, and -10) HDACs are Zn^{2+}-dependent lysine deacetylases and are inhibited by canonical HDAC inhibitors.[4] Unlike classes I and II, class III HDACs (sirtuins) are Zn^{2+}-independent lysine deacetylases that require NAD^+ as a cofactor and are not inhibited by a canonical HDAC inhibitor.[5] Class IV (HDAC11) has a very poor sequence homology with other HDACs.[6]

HDACs are high-priority drug targets for the treatment of various human diseases, including cancer.[7,8] Different HDAC isozymes are overexpressed in various forms of human cancers.[9] Inhibitors of HDACs are known to cause an anticancer effect both *in vitro* and in a xenograft animal model.[10] The HDAC inhibitors, namely, SAHA and romidepsin, have already been approved by the Food and Drug Administration for the treatment of T-cell lymphoma. Moreover, several others HDAC inhibitors are in the advanced stage of clinical trials.[11] However, the currently known inhibitors of HDAC produce severe side effects on cancer patients, presumably because they indiscriminately targets several HDAC isozymes, many of which are vital for normal physiological processes. Thus, there has been an ongoing effort to develop and design an alternative that would show better *in vivo* efficacy.[12]

The inhibition constant (K_i) and the equilibrium dissociation constant (K_d) of an HDAC inhibitor often do not correlate with its *in vivo* efficacy. For instance, the *in vitro* potency of TSA against human HDACs is several-fold higher than that of

Received: June 11, 2013
Revised: September 3, 2013
Published: September 30, 2013

   dx.doi.org/10.1021/bi400740x | *Biochemistry* 2013, 52, 8139−8149

SAHA, but the latter inhibitor shows a better efficacy in the clinical settings.[13] It is widely known that the physicochemical (Lipinski parameters) as well as the ADME (absorption, distribution, metabolism, and excretion) properties of a drug candidate play significant roles in defining its *in vivo* efficacy.[14,15] The hydroxamate-based HDAC inhibitors, such as TSA and SAHA, reportedly do not exhibit optimal physiochemical and ADME properties.[16,17] Interestingly, even the structurally similar compounds could have a marked difference in their ADME properties.[17] A poor oral bioavailability of SAHA could be conceived from the fact that its linker domain contains an amide moiety, which is likely to reduce the oral bioavailability of the drug because of a strong hydrogen bonding interaction with water molecules.[18] On the other hand, poor bioavailability of TSA could be partly correlated with the nonrotatable bonds of its linker domain. The latter feature reduces the molecular flexibility, an important parameter that has been proposed to be positively correlated with membrane permeability and bioavailability.[19]

Aside from the ADME properties, the therapeutic efficacies of certain drugs have been correlated with the transient kinetic and thermodynamic parameters of the protein−ligand complexes.[20,21] Markgrenn and co-workers have investigated the significance of k_{on} and k_{off} of the drug−target interaction in determining the therapeutic efficacy of HIV protease inhibitors.[22] Copeland et al. have extensively reviewed the influence of the residence time of the receptor−ligand complex on various biological functions.[23,31] Likewise, Davis and colleagues reported that the downstream biological effects of a peptide serving as an agonist or antagonist of the TCR−MHC complex are dictated by the kinetic parameters of the receptor−ligand inteaction.[24] Furthermore, Freire and other investigators suggest that the thermodynamic parameters for the drug−target interaction could be utilized as a complementary tool for lead optimization to enhance the therapeutic efficacy of a drug.[21,25,26] In view of these literature precedents, it appeared logical to investigate the detailed kinetic and thermodynamic features of the binding of structurally similar ligands, SAHA and TSA, to the recombinant form of human HDAC8. Our experimental data provide the kinetic and thermodynamic rationale for SAHA being the target-specific and -selective inhibitor of HDAC8 as compared to its structurally similar counterpart, TSA.

MATERIALS AND METHODS

TSA was purchased from Enzo Life Sciences (Farmingdale, NY). SAHA (suberoylanilide hydroxamic acid) was custom synthesized by Biomol Laboratories (Plymouth Meeting, PA). Coumarin-SAHA (c-SAHA) was synthesized in our laboratory as described previously.[27] A recombinant form of human HDAC8 was purified from *Escherichia coli* as described previously.[27]

Equilibrium Binding Studies of HDAC8−Inhibitor Interactions. All the steady-state spectrofluorometric studies were performed in protein storage buffer [50 mM Tris (pH 7.5) containing 100 mM NaCl, 3 mM $MgCl_2$, 10% glycerol, and 1 mM tris(2-carboxyethyl)phosphine (TCEP)] on a Perkin-Elmer Lambda 50-B spectrofluorometer that was equipped with a magnetic stirrer and a thermostated water bath using a 4 mm × 4 mm quartz cuvette. The change in the intrinsic fluorescence signal of HDAC8 upon binding of an inhibitor was used to obtain the binding isotherm of the enzyme−inhibitor complex. To determine the equilibrium dissociation constant of an inhibitor for HDAC8, a fixed concentration of HDAC8 (1.5 μM) was titrated with an increasing concentration of the respective inhibitor in protein storage buffer. The fluorescence emission spectrum of HDAC8 was monitored at 340 nm after excitation at 295 nm. The resulting binding isotherms for the HDAC8−inhibitor complex were analyzed via the complete solution of the quadratic equation (eq 1).

$$F = C(I_{tot} + K_d + nE_{tot}) - \{[(E_{tot}n + I_{tot} + K_d)^2 - 4E_{tot}nI_{tot}]^{1/2}\}/2 \quad (1)$$

where F is the fluorescence signal of the protein−ligand species after the addition of the inhibitor, E_{tot} and I_{tot} refer to the total enzyme and total inhibitor concentrations, respectively, K_d is the equilibrium dissociation constant of the enzyme−inhibitor complex, n is the stoichiometry of the enzyme−inhibitor complex, and C is the change in the amplitude of the signal.

Transient Kinetics of HDAC8−Ligand Interaction. To determine the rate constants of binding as well as dissociation of HDAC8 inhibitors from the enzyme's site, transient kinetic experiments were performed using an Applied Photophysics SX-18MV stopped-flow system. The stopped-flow system described above, which has a dead time of 1.3 ms, was operated in fluorescence mode with an emission path length of 2 mm. The time-dependent decrease in the intrinsic HDAC8 fluorescence was monitored by exciting the reaction mixture at 280 nm using a 320 nm cutoff filter. All of the transient kinetic experiments were performed at least 10 times in 50 mM Tris buffer (pH 7.5) containing 100 mM NaCl and 1 mM TCEP. The resultant kinetic traces were averaged and analyzed by the data analysis package provided by Applied Photophysics. For association kinetics, all the experiments were performed under pseudo-first-order conditions. The kinetic traces were analyzed using single- and double-exponential rate equations (eqs 2 and 3) as follows.

$$\text{RFU} = \text{Amp}\exp(-k_{obs}t) + \text{offset} \quad (2)$$

where RFU is the fluorescence signal at a given time and Amp and k_{obs} are the total amplitude and observed rate constant, respectively.

$$\text{RFU} = \text{Amp}_1\exp(-k_{obs1}t) + \text{Amp}_2\exp(-k_{obs2}t) + \text{offset} \quad (3)$$

where RFU represents the fluorescence signal at a given time and Amp_1 and Amp_2 are the amplitudes associated with observed rate constants k_{obs1} and k_{obs2}, respectively. Observed rate constants were measured as a function of ligand concentration, and data were analyzed using appropriate kinetic models as described in subsequent sections.

Determination of the Rate of Dissociation of HDC8−Inhibitor Complexes. The rates of dissociation (k_{off}) of TSA and SAHA from the enzyme's site were determined utilizing a fluorescent analogue of SAHA, coumarin-SAHA (c-SAHA), as the displacing ligand. Competitive binding of c-SAHA to HDAC8 (concomitant with displacement of the enzyme-bound nonfluorescent inhibitor) results in a decrease in the fluorescence signal at 400 nm (λ_{ex} = 325 nm).[27] The time-dependent change in the fluorescence signal was used to measure the dissociation rate of the enzyme−inhibitor complex. Scheme 1 outlines the principle involved in determining the rate of dissociation of the HDAC8−inhibitor complex.

When the HDAC8−TSA/SAHA complex is mixed with an excessive concentration of c-SAHA, the mass action drives the

dx.doi.org/10.1021/bi400740x | *Biochemistry* 2013, 52, 8139−8149

Scheme 1. Measurement of the Rate of Dissociation of the HDAC8−Inhibitor Complex

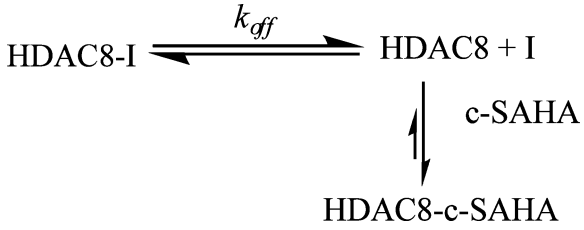

overall equilibrium toward the enzyme−c-SAHA complex. It is important to note that the association kinetics of c-SAHA is several fold faster than that of SAHA (our unpublished results). Under the conditions described above, the rate of formation of the HDAC8−c-SAHA complex is given by the dissociation rate of the inhibitor. The dissociation rate of the inhibitor was measured by mixing 1 μM HDAC8 and 20 μM inhibitor (syringe I) with 100 μM c-SAHA (syringe II) via the stopped-flow system and monitoring the time-dependent decrease in the fluorescence signal (λ_{ex} = 325 nm; 395 nm cutoff filter) due to formation of the HDAC8−c-SAHA complex. The data were analyzed using a single-exponential rate equation with a data analysis software package provided by Applied Photophysics.

Temperature Dependence of Transient Kinetic Measurements. The temperature-dependent transient kinetic experiments were performed to delineate the energetics of the ligand−protein interaction utilizing the stopped-flow system. The experimental temperature was maintained using a circulating water bath. The observed rate constant and the rate constants associated with the transient kinetic of binding and dissociation of the ligand were determined at different temperatures, and they were analyzed with the Arrhenius equation (eq 4).

$$1/k_{obs} \text{ or } 1/k = A \exp[-E_a/(RT)] \quad (4)$$

where k_{obs} and k are the observed rate constant and the rate constant obtained from transient kinetic experiments, respectively, A is the frequency factor, E_a is the Arrhenius activation energy, and T is the temperature in kelvin. To convert E_a into the transition-state enthalpy ($\Delta H^{\ddagger}$), the following relationship was used (eq 5).

$$\Delta H^{\ddagger} = E_a - RT \quad (5)$$

The activation free energy ($\Delta G^{\ddagger}$) was calculated using the Eyring equation (eq 6).

$$\Delta G^{\ddagger} = -RT \ln(kh/k_B T) \quad (6)$$

where R is the gas constant (1.986 cal K^{-1} mol^{-1}), T is the absolute temperature, h is Planck's constant (1.58×10^{-34} cal s), and k_B is Boltzmann's constant (3.3×10^{-24} cal K^{-1}).

Isothermal Titration Calorimetry (ITC) Studies. The enthalpy (ΔH°) of binding of TSA and SAHA to HDAC8 was determined by performing isothermal titration calorimetric experiments on a VP-ITC instrument (Microcal Inc., Northampton, MA). The enzyme and inhibitor solutions were properly degassed under vacuum. The ITC sample cell was filled with 1.8 mL (effective volume of 1.4 mL) of 10 μM HDAC8 in 50 mM Tris (pH 7.5) containing 100 mM NaCl, 3 mM $MgCl_2$, 10% glycerol, and 1 mM TCEP. HDAC8 was titrated with 45 aliquots (4 μL each) of TSA or SAHA prepared in HDAC8 dialysis buffer. The reaction mixture was continuously stirred at 250 rpm during the calorimetric titration. Raw experimental data were obtained as the amount of heat produced per second upon addition of the ligand to the sample cell. The magnitude of heat produced per injection was calculated by the integration of the area under individual peaks using Origin software, provided with the ITC instrument. The observed heat signal in each injection was due to the heat associated with binding and the background signal that was mainly due to the heat of dilution. The heats of dilution determined in the control experiments were essentially similar to the heat signal obtained at the end of the titration; so the average signal of the last five injections was used as the background heat signal. The final data were presented as the amount of heat produced per injection as a function of the molar ratio of the ligand. The data were analyzed using Origin (available from Microcal), as described previously by Wiseman et al.,[28] yielding the stoichiometry (n), the association constant (K_a), and the standard enthalpy change (ΔH°) for the binding of an inhibitor to HDAC8.

RESULTS

In a cursory manner, we observed that the intrinsic fluorescence of HDAC8 is quenched upon its binding to various enzyme inhibitors, including TSA and SAHA. Figure 1 shows the steady-state emission spectrum of 1.5 μM HDAC8 in 50 mM Tris-HCl (pH 7.5) containing 100 mM NaCl, 3 mM $MgCl_2$, 10% glycerol, and 1 mM TCEP upon excitation at 295 nm. HDAC8 showed the fluorescence emission maximum (λ_{max}) of 340 nm. Binding of an inhibitor (TSA or SAHA) led to the quenching of HDAC8's intrinsic fluorescence without any shift in the emission maximum (Figure 1). To probe the mechanism of fluorescence quenching in the cases described above, we performed the excited-state lifetime measurement of HDAC8's tryptophan residues. The experimental data revealed that fluorescence lifetime of the enzyme's tryptophan did not change upon binding of TSA or SAHA, suggesting the fluorescence quenching is "static" (rather than "dynamic") in nature (data not shown).

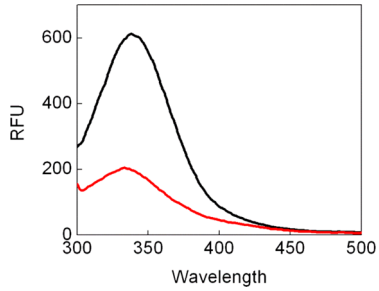

Figure 1. Steady-state fluorescence emission spectra (black) of 1.5 μM HDAC8 upon excitation at 295 nm. The intrinsic fluorescence of HDAC8 is quenched (red) upon binding to TSA.

The equilibrium binding study of an inhibitor to HDAC8 was pursued utilizing the change in HDAC8's fluorescence signal upon ligand binding. Figure 2 shows the titration of a fixed concentration of HDAC8 (1.5 μM) with an increasing concentration of the inhibitor. The fluorescence intensity of HDAC8 at 340 nm, which is dependent on its fractional occupancy of an inhibitor, is hyperbolically dependent on the inhibitor concentration. During the course of the titration, the concentration of HDAC8 was comparable to that of the

dx.doi.org/10.1021/bi400740x | Biochemistry 2013, 52, 8139−8149

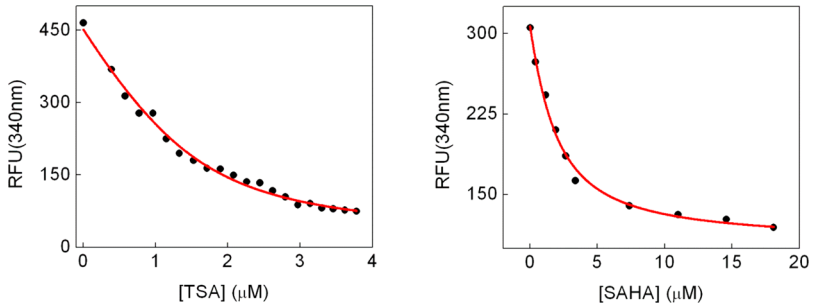

Figure 2. Binding isotherms for the interaction of TSA (left) and SAHA (right) with HDAC8. The decrease in the intrinsic fluorescence of HDAC8 at 340 nm (λ_{ex} = 295 nm) has been plotted as a function of an increasing concentration of the respective ligand. The solid lines are the best fits of the experimental data, yielding K_d values of 0.39 ± 0.08 and 1.2 ± 0.2 μM for TSA and SAHA, respectively.

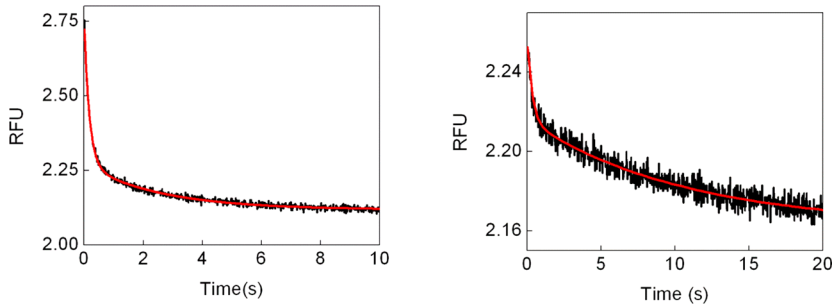

Figure 3. Representative stopped-flow kinetic traces for the binding of TSA (left) and SAHA (right) to HDAC8. The solid smooth lines represent the best fits of the data for inhibitor binding according to the double-exponential rate equation, yielding fast and slow observed rate constants of 5.58 ± 0.09 and 0.21 ± 0.01 s^{-1}, respectively, for TSA binding. The corresponding values for SAHA binding were 2.78 ± 0.31 and 0.087 ± 0.043 s^{-1}, respectively.

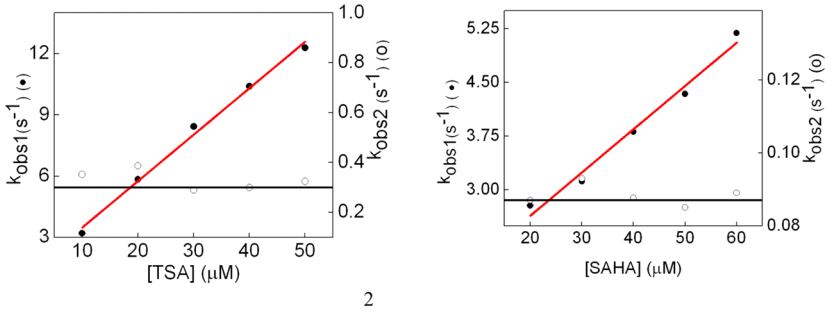

Figure 4. Concentration dependence of the observed rate constants for the binding of TSA (left) and SAHA (right) to HDAC8. A linear regression line to the data (●) for TSA binding provides a gradient (k_{+1}) and an intercept (k_{-1}) of 2.2 × 10^5 M^{-1} s^{-1} and 1.2 s^{-1}, respectively, whereas the horizontal line shows the best fit of the data (○) providing a k_{obs2} (=k_{+2} + k_{-2}) of 0.37 s^{-1}. A linear regression line to the data (●) for SAHA binding provides a gradient (k_{+1}) and an intercept (k_{-1}) of 6 × 10^4 M^{-1} s^{-1} and 1.4 s^{-1}, respectively. The horizontal line shows the best fit of the data (○) providing a k_{obs2} (=k_{+2} + k_{-2}) of 0.089 s^{-1}.

inhibitor; hence, the binding isotherms were analyzed by a complete solution of the quadratic equation (eq 1), yielding equilibrium dissociation constants (K_d) for the binding of TSA and SAHA of 0.39 ± 0.08 and 1.2 ± 0.2 μM, respectively. We further determined the K_i (inhibition constant) values of TSA and SAHA using the protocol as described previously by our group[27] to be 0.15 ± 0.02 and 0.45 ± 0.11 μM, respectively. Note the similarity between the K_d and K_i values for both ligands, suggesting that the inhibition or the quenching of the intrinsic HDAC8's fluorescence is due to the binding of the ligands to the enzyme active site. Furthermore, our experimental data suggest that HDAC8 has only one binding site for TSA, and the second TSA molecule bound to HDAC8, which has been previously observed in crystallographic studies, is presumably due to crystallization conditions.[29]

Transient Kinetic Studies of Inhibitor Binding. To determine the kinetic mechanism of binding of an inhibitor to HDAC8, we performed transient kinetic experiments using the stopped-flow system. Figure 3 (left panel) shows the representative stopped-flow kinetic trace for the association of TSA with HDAC8 obtained upon mixing of 1 μM HDAC8 with 10 μM TSA via the stopped-flow syringes. The change in the intrinsic fluorescence of HDAC8 due to the binding of the inhibitor was monitored upon exciting the mixture at 280 nm and using a 330 nm cutoff filter. The kinetic trace was analyzed with a double-exponential rate equation, yielding fast (k_{obs1}) and slow (k_{obs2}) observed rate constants of 5.58 ± 0.09 and 0.21 ± 0.01 s^{-1}, respectively. We performed a similar stopped-flow transient kinetic experiment for the binding of SAHA to HDAC8. Figure 3 (right panel) shows the representative stopped-flow kinetic trace for the association of SAHA with

dx.doi.org/10.1021/bi400740x | Biochemistry 2013, 52, 8139−8149

Scheme 2. Two-Step Mechanism of Binding of HDAC8 Inhibitors to the Enzyme

$$\text{HDAC8} + \text{I} \underset{k_{-1}}{\overset{k_{+1}}{\rightleftharpoons}} \text{HDAC8-I}^{*} \underset{k_{-2}}{\overset{k_{+2}}{\rightleftharpoons}} \text{HDAC8-I}^{**}$$

Bimolecular Step Isomerization Step

$$k_{obs1} = k_{+1}[\text{I}] + k_{-1} \qquad k_{obs2} = k_{+2} + k_{-2}$$

HDAC8 obtained upon mixing of 1 μM HDAC8 with 20 μM SAHA via the stopped-flow syringes. The kinetic trace was analyzed with a double-exponential rate equation, yielding fast (k_{obs1}) and slow (k_{obs2}) observed rate constants of 2.78 ± 0.31 and 0.087 ± 0.043 s^{-1}, respectively. Note that the magnitude of both the fast and slow observed rate constants for the binding of TSA to HDAC8 is higher than the magnitude of those of SAHA, suggesting that the association kinetics of the former ligand is faster than the latter.

To delineate the microscopic pathways for the binding of the inhibitor to HDAC8, we measured the observed rate constants as a function of inhibitor concentration. Figure 4 shows the concentration dependence of the observed rate constant (k_{obs}) for the binding of TSA and SAHA to HDAC8 (left and right panels, respectively). Note that while the magnitude of the fast observed rate constant (k_{obs1}) is linearly dependent on the ligand concentration, the slow observed rate constant (k_{obs2}) essentially remains constant. This observation is similar to what has been observed for the binding of TA-calmodulin to myosin muscle myosin light chain kinase by Trentham and collaborators.[30] The data were analyzed in light of a two-step binding mechanism (Scheme 2).

In the binding mechanism depicted in Scheme 2, the fast phase (bimolecular step) is likely to be due to the initial binding or encounter of the inhibitor (I) with the enzyme site, whereas the slow phase (isomerization) could be attributed to the isomerization of the transient encounter complex (HDAC8−I*) to produce the final reaction product (HDAC8−I**). Constants k_{+1}, k_{-1}, k_{+2}, and k_{-2} are the rate constants of the association reaction. The linear regression analysis of the data for k_{obs1} with the gradient and intercept provides values of k_{+1} and k_{-1}, which were found to be 2×10^5 M^{-1} s^{-1} and 1.2 s^{-1}, respectively, for TSA binding. The corresponding values of these kinetic parameters for SAHA binding were 6×10^4 M^{-1} s^{-1} and 1.4 s^{-1}, respectively. Evidently, the second-order rate constant for the bimolecular (k_{+1}) step is 1 order of magnitude greater for binding of TSA to HDAC8 than for binding of SAHA. The value of k_{obs2}, which is representative of the isomerization step, is independent of ligand concentration, and it is comprised of the sum of k_{+2} and k_{-2}.

Dissociation Rate (k_{off}) of HDAC8 Inhibitors. We determined the dissociation rates (k_{off}) for dissociation of TSA and SAHA from the enzyme's site utilizing coumarin-SAHA (c-SAHA) as a fluorescent probe. c-SAHA serves as a competitive ligand that triggers the dissociation of the nonfluorescent inhibitors (e.g., TSA and SAHA), when utilized at an excessively high concentration. Figure 5 shows the stopped-flow kinetic trace for the dissociation of TSA from the enzyme's site, which was obtained by mixing a solution

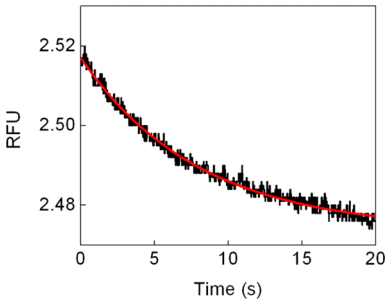

Figure 5. Representative stopped-flow trace for the dissociation of TSA from HDAC8's active site. The dissociation of the enzyme-bound TSA was triggered by the mixing of the HDAC8−TSA complex with a high concentration of c-SAHA. The solid smooth line is the best fit of the experimental data according to the single-exponential rate equation, yielding a dissociation rate for TSA of 0.11 ± 0.02 s^{-1}.

containing 1 μM HDAC8 and 20 μM TSA with 100 μM c-SAHA via the stopped-flow syringes. The solid line is the best fit of the experimental data using the single-exponential rate equation, yielding a k_{off} for TSA of 0.11 s^{-1}. The k_{off} of SAHA has been previously reported by our group to be 0.41 s^{-1}, which is 4-fold higher than that of TSA.[27] For the kinetic model of the ligand−protein interaction described in Scheme 2, the k_{off} of the ligand is given by eq 7.[30]

$$k_{off} = (k_{-1}k_{-2})/k_{+2} \tag{7}$$

Taking into account the magnitudes of the dissociation rates (k_{off}) of TSA and SAHA as well as the observed rate constants (k_{obs}) of their association reactions, we could deduce the values of all four constants (k_{+1}, k_{-1}, k_{+2}, and k_{-2}) and thereby predict the value of equilibrium dissociation constant (K_d) for the binding of the inhibitors mentioned above. The equilibrium dissociation constants of TSA and SAHA deduced from the transient kinetic experiments were 0.49 and 6.8 μM, respectively. Note that these values are in close agreement (within experimental error) with the directly measured K_d values determined via a direct titration of the enzyme with the inhibitors determined from the steady-state experiments (Table 1). The similarity between the directly determined and kinetically calculated K_d values validates the authenticity of the two-step binding mechanism of TSA and SAHA with HDAC8.

Temperature Dependence of Association Kinetics. To determine the energetic contributions for the binding of TSA and SAHA to HDAC8 in ground and putative transition states, we performed the temperature-dependent stopped-flow experiments. Figure 6 shows the temperature dependence of the observed rate constants for the association of TSA and SAHA. The fast observed rate constant (k_{obs1}) increases as a function of

dx.doi.org/10.1021/bi400740x | Biochemistry 2013, 52, 8139−8149

Table 1. Comparison of K_d Values Calculated via the Transient Kinetic Method with Spectrofluorometric Titration

ligand	k_{+1} (M^{-1} s^{-1})	k_{-1} (s^{-1})	k_{+2} (s^{-1})	k_{-2} (s^{-1})	K_d (μM) (kinetic method)	K_d (μM) (spectrofluorometric titration method)
TSA	2.3×10^5	1.2	0.34	0.03	0.49	0.39 ± 0.08
SAHA	6.0×10^4	1.4	0.069	0.02	6.8	1.2 ± 0.2

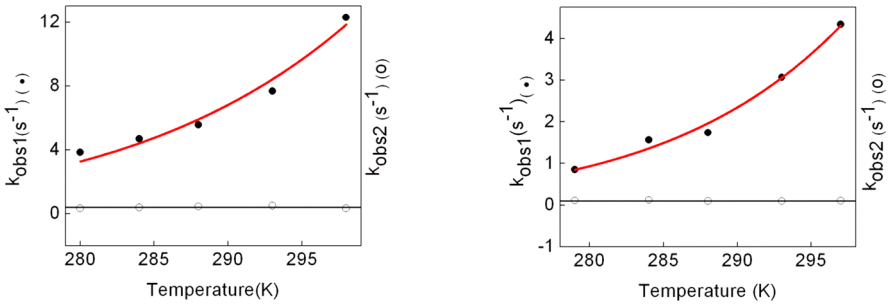

Figure 6. Temperature dependence of the observed rate constants for the bimolecular and isomerization steps of the interaction of HDAC8 with TSA and SAHA. The Arrhenius activation energies (E_a) for the bimolecular step for TSA (left) and SAHA (right) were calculated from the best fit of the experimental data using the Arrhenius equation to be 12 and 15 kcal/mol, respectively. The isomerization step has zero activation energy.

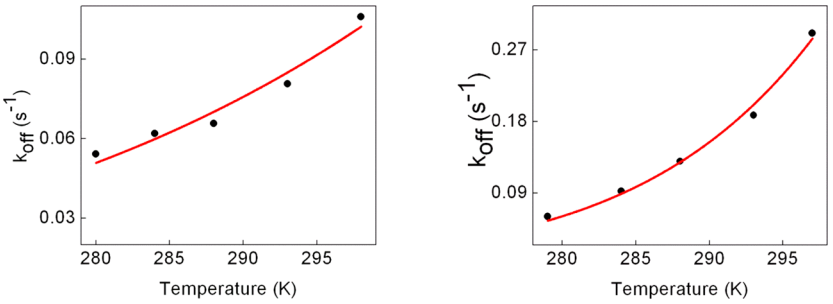

Figure 7. Arrhenius plots for the observed dissociation rate of TSA and SAHA measured using c-SAHA. The solid lines are the best fits of the experimental data using the Arrhenius equation with activation energies of 5.6 and 12.8 kcal/mol for TSA (left) and SAHA (right), respectively.

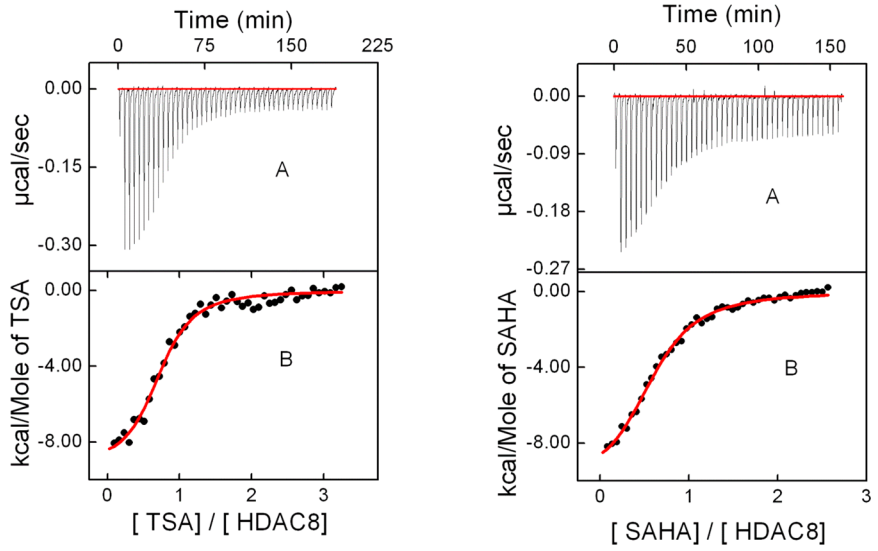

Figure 8. ITC profile for the binding of TSA (left) and SAHA (right). Panel A shows the calorimetric data. The solid smooth lines in panel B represent the best fits of the experimental data yielding the thermodynamic parameters of ligand binding listed in Table 2.

temperature, whereas k_{obs2} essentially remains constant for the binding of both inhibitors. The activation energy of the bimolecular step of the ligand−protein interaction was calculated using the Arrhenius equation (eq 4). The activation energies (E_a) for the biomolecular step (fast phase) of binding of TSA and SAHA to HDAC8 were 12 and 15 kcal/mol, respectively. Note that the activation energy for the association of SAHA is 3 kcal/mol higher than that of TSA.

We further investigated the effect of temperature on the forward and reverse rate constants associated with the biomolecular step, i.e., k_{+1} and k_{-1}, respectively. The energy of activation was calculated from the temperature dependence of k_{+1} and k_{-1} for the binding of TSA and SAHA. The energies

dx.doi.org/10.1021/bi400740x | Biochemistry 2013, 52, 8139−8149

Table 2. Summary of the Thermodynamic Parameters for the Binding of TSA and SAHA to HDAC8 at 25 °C

inhibitor	$\Delta G°$ (kcal/mol)	$\Delta H°$ (kcal/mol)	$T\Delta S°$ (kcal/mol)	K_a (M^{-1})	stoichiometry
SAHA	−8.4	−10.9 ± 0.15	−2.5	8.1×10^5	0.71
TSA	−8.6	−8.9 ± 0.12	−0.3	1.67×10^6	0.82

Figure 9. Closer view of the active site pocket of HDAC8 bound with TSA and SAHA. The dimethylaniline moiety of TSA makes a $\pi-\pi$ interaction the Y100 residue of HDAC8 [Protein Data Bank (PDB) entry 1T64]. The Asp101 residue of HDAC8 makes a specific hydrogen bond with the connector group of SAHA (PDB entry 1T69).

of activation (E_a) for the forward and reverse steps of the bimolecular step for the binding of TSA were 9.3 and 13.5 kcal/mol, respectively. The corresponding values of the activation parameters mentioned above for SAHA binding were 11.4 and 18.5 kcal/mol, respectively. Evidently, the activation energy (E_a) for both the forward and reverse reactions of the bimolecular step for SAHA binding is higher than that of TSA, which accounts for the fact that the kinetics of association of SAHA to HDAC8 is slower.

Temperature Dependence of the Rate of Dissociation (k_{off}) of TSA and SAHA from HDAC8's Active Site. In view of delineating the energetics of dissociation of TSA and SAHA from HDAC8's active site, we measured the dissociation rates at different temperatures ranging from 5 to 25 °C. Figure 7 shows the Arrhenius plots for k_{off} of TSA and SAHA. The solid lines are the best fit of the experimental data according to the Arrhenius equation (eq 4), with activation free energies (E_a) of 6.4 and 15 kcal/mol, respectively, for the dissociation of TSA and SAHA from the enzyme's active site. Note that the activation energy (E_a) for the dissociation of SAHA is ∼2-fold higher than that of TSA. Although the activation energy (E_a) for the dissociation of TSA is ∼2-fold lower than that of SAHA, its dissociation rate (k_{off}) at 25 °C is 4-fold lower. Evidently, enthalpic and entropic changes associated with the formation of the ground and putative transition states of the enzyme−inhibitor complex prior to the dissociation of the inhibitors mentioned above from HDAC8's active site are significantly different.

Isothermal Titration Calorimetry (ITC) Studies of the Binding of TSA and SAHA. To measure the calorimetric enthalpy for the binding of TSA and SAHA to HDAC8, we performed ITC experiments (Materials and Methods). Figure 8 shows the titration of 10 μM HDAC8 with 45 injections (4 μL each) of 200 μM inhibitor (TSA or SAHA) in 50 mM Tris buffer (pH 7.5) containing 100 mM NaCl, 3 mM $MgCl_2$, 10% glycerol, and 1 mM TCEP at 25 °C. Figure 8A shows the raw calorimetric data, representing the amount of heat produced (negative exothermic peaks) following each injection of inhibitor. The area under each peak represents the amount of heat produced upon binding of the inhibitor to HDAC8. Figure 8B shows the plot of the amount of heat generated per injection as a function of the molar ratio of the ligand to the enzyme. The smooth lines represent the best fit of the experimental data according to the equation described by Wiseman et al.,[28] yielding thermodynamic parameters for the binding of TSA and SAHA to HDAC8 (see Table 2). The $\Delta H°$

dx.doi.org/10.1021/bi400740x | Biochemistry 2013, 52, 8139−8149

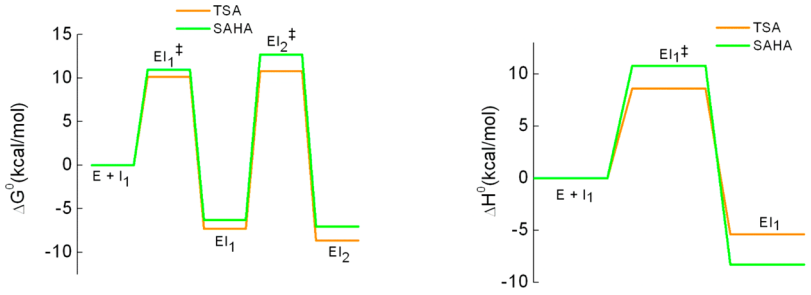

Figure 10. Free energy (left) and enthalpy (right) profiles for the binding of TSA and SAHA. The free energies and the enthalpies of the enzyme and the ligand were taken to be equal to zero.

values for the binding of SAHA and TSA to HDAC8 were −10.9 ± 0.15 and −8.9 ± 0.12 kcal/mol, respectively. Evidently, ΔH° for the binding of SAHA is 2 kcal/mol higher than that for binding of TSA to HDAC8. Furthermore, the entropic penalty for the binding of TSA measured at 25 °C is 10-fold smaller than that of SAHA.

DISCUSSION

With our observation that the intrinsic fluorescence of HDAC8 is quenched upon binding of an inhibitor, we could investigate the detailed transient kinetic mechanism for the interaction of two structurally similar inhibitors, TSA and SAHA, with the recombinant form of human HDAC8. The experimental data presented herein revealed the following salient features of the association and dissociation kinetics of these ligands. The association of both TSA and SAHA with HDAC8 conformed to two kinetically resolvable steps, i.e., the first (bimolecular) step leading to the formation of the transient enzyme−inhibitor complex followed by the second isomerization step (Scheme 2). The first (bimolecular) step is faster than the isomerization in both cases. Even though TSA and SAHA are structurally similar ligands, their association and dissociation kinetics are markedly different. The kinetics of binding of TSA to HDAC8 is faster than that of SAHA, whereas the rate of dissociation of TSA from the enzyme's active site is 4 times slower. Whereas the first (bimolecular) step for the binding of both inhibitors is primarily contributed by enthalpic changes, the isomerization step is solely given by entropic changes. The standard binding enthalpy (ΔH°) of SAHA derived from the transient kinetic as well as the isothermal titration experiments is approximately 2−3 kcal/mol higher than that given by TSA.

HDAC8 contains four tryptophan residues, of which two are partially exposed to the bulk solvent.[29] The ligand-induced conformational change in HDAC8 due to the binding of an inhibitor would alter the microenvironment of the tryptophan residues mentioned above, resulting in quenching of the intrinsic protein fluorescence. Furthermore, the excited-state lifetime of the HDAC's tryptophan remained the same upon binding to TSA or SAHA, suggesting that the inhibitor forms a ground-state complex with tryptophan, which is nonfluorescent in nature.

It is important to note that the equilibrium dissociation constants (K_d) for the binding of TSA and SAHA to HDAC8 deduced from the transient kinetic experiment are in the close agreement (within experimental error) with the values obtained via the equilibrium binding experiments (Table 1), validating the authenticity of the proposed kinetic model (Scheme 2). The forward rate constants, k_{+1} and k_{+2}, for the interaction of TSA with HDAC8 are 1 order of magnitude higher than those of SAHA. We believe that the origin of this feature lies in the structural differences between SAHA and TSA (Figure 9) and their mode of interaction with HDAC8. Note that the dimethylaniline moiety of TSA makes a $\pi-\pi$ interaction with the Y100 residue of HDAC8 (see the left panel of Figure 9).[29] This feature would facilitate the proper orientation of the binding partners, thus enhancing the magnitude of the forward rate constants (k_{+1} and k_{+2}) for the binding of TSA to HDAC8. On the other hand, the reverse rate constants for the initial binding (k_{-1}) and the isomerization of the enzyme−inhibitor complex (k_{-2}) are similar in magnitude for both ligands. A comparative account of the experimentally determined K_d values and the microscopic rate constants for the binding of these ligands to the enzyme reveals that the isomerization step plays an important role in enhancing the binding affinity of both TSA and SAHA to HDAC8; albeit, it is more pronounced in the former case. We measured the dissociation rates of TSA and SAHA utilizing a fluorescent analogue of SAHA, coumarin-SAHA. The magnitude of the rate of dissociation (k_{off}) of the inhibitor from the enzyme's site is dependent on the value of three rate constants, k_{-1}, k_{-2}, and k_{+2} [$k_{off} = k_{-1}k_{-2}/k_{+2}$ (eq 7)]. Because the forward isomerization rate constant (k_{+2}) for the interaction of TSA with HDAC8 is 1 order of magnitude higher than that of SAHA, the former ligand dissociates slower (4-fold) from the enzyme's active site. The fast dissociation of SAHA from HDAC8 can be suggested to decrease the resident time of the enzyme−SAHA complex in the physiological system, and such a feature has the potential to obviate undesirable side effects associated with an extended downstream cell signaling process.[32]

We further delineated the energetic profiles of the enzyme−inhibitor interactions by performing temperature-dependent transient kinetic studies (see Figure 10). The microscopic rate constants for the binding of both TSA and SAHA were determined, and they were translated into the energy of individual components (see Table 3). The data in Table 3 were utilized to construct the energy diagrams for the binding of TSA and SAHA to HDAC8 (Figure 10). The free energy diagrams shown in Figure 10 (left panel) reveal that the ΔG° values for the formation of the enzyme−inhibitor encounter complex and the subsequent isomerization step are ∼0.9 and ∼0.7 kcal/mol more favorable, respectively, for TSA than for SAHA. In addition, the putative transition states ($\Delta G^{\ddagger}$) for the formation of the encounter and isomerized complexes are 0.8 and 1.1 kcal/mol more favorable, respectively, for TSA than for SAHA. Clearly, as compared to TSA, SAHA requires more structural adjustments with the enzyme's active site pocket to attain the encounter and isomerized complexes, implying that

dx.doi.org/10.1021/bi400740x | Biochemistry 2013, 52, 8139−8149

Table 3. Transient Kinetic Parameters for the Interaction of TSA and SAHA with HDAC8

parameter [energy (kcal/mol)]	TSA	SAHA
ΔG° (overall)	−8.5	−7.0
ΔG° (k_{-1}/k_{+1})	−7.2	−6.3
$\Delta G^{\ddagger}_{k_{+1}}$	10.1	10.9
$\Delta H^{\ddagger}_{k_{+1}}$	8.6	10.8
$\Delta G^{\ddagger}_{k_{-1}}$	17.3	17.2
$\Delta H^{\ddagger}_{k_{-1}}$	14.0	19.1
ΔH° (k_{-1}/k_{+1})	−5.4	−8.3
$T\Delta S^\circ$ (k_{-1}/k_{+1})	1.8	−2.0
ΔG° (k_{-2}/k_{+2})	−1.4	−0.7
$\Delta G^{\ddagger}_{k_{+2}}$	18.1	19.0
$\Delta G^{\ddagger}_{k_{-2}}$	19.5	19.7

the latter ligand (SAHA) makes more specific interactions with the enzyme. Note that the linker moiety of TSA is shorter, bulkier, and more rotationally constrained than SAHA (Figure 9). We believe that the rotational flexibility and hydrophobicity of SAHA (vis-à-vis TSA), as well as the entropic penalty associated with the HDAC8−SAHA interaction, are responsible for the energetic unfavorability. The thermodynamic signature (ΔG° and ΔH°) described above for SAHA binding is likely to enhance the specificity and selectivity of binding of SAHA to HDAC8. However, the energetic constraints described above are more favorable for the dissociation of SAHA from the enzyme's active site because of the high entropic favorability. It is important to note that the Arrhenius activation energy (E_a) for the observed dissociation (k_{off}) of SAHA from the enzyme's active site is ∼2-fold higher than that of TSA (Figure 7), suggesting that the HDAC8−SAHA complex requires more heat energy ($\Delta H/E_a$) to reach the putative transition state prior to the complete dissociation of the ligand from the target site. Thus, a higher value of E_a for the observed dissociation of SAHA from the enzyme site further attests to the fact that it makes more specific interactions with the enzyme than TSA does.

By determining the temperature-dependent microscopic parameters for the binding of TSA and SAHA to HDAC8, we could dissect the enthalpic contributions from the overall free energy changes in the ground and putative transition states for the respective complexes. Because the values of k_{+2} and k_{-2} for the binding of TSA and SAHA are independent of temperature, it is tempting to propose that the isomerization step is entropically driven. Hence, the enthalpic contribution in the ground and putative transition states is realized up to the formation of the enzyme−ligand encounter complexes. The enthalpy diagram (see Figure 10, right panel) clearly shows that whereas SAHA (vis-à-vis TSA) has to cross a higher enthalpic barrier in the forward and reverse directions, it is enthalpically more stable in the ground state of the enzyme−inhibitor encounter complex. A qualitatively similar conclusion is derived from the isothermal titration calorimetric studies for the binding of SAHA versus that of TSA (Figure 8). It is important to note the ΔH° for the binding of TSA as well as SAHA to HDAC8 directly measured via ITC is approximately 2−3 kcal/mol higher than the kinetically derived ΔH° (see Tables 2 and 3). We believe the origin of this discrepancy lies in the fact that the kinetically derived ΔH° is essentially the measure of van't Hoff enthalpy, which in many cases differs from the directly measured calorimetric enthalpy.[33]

It is important to note that the molecular origin as well as the structural parametrization of ΔH° of a biomolecular interaction is often complex.[34] However, the thermodynamic studies for the binding of structurally similar ligands to a common target in conjunction with their crystallographic studies suggest that a higher (negative) binding enthalpy (ΔH°) is primarily linked with the specific interactions (such as hydrogen bonding) between the binding partners. For instance, the HIV protease and HMG CoA inhibitors containing a high binding enthalpy for the target have been found to be more target-specific and -selective and reportedly serve as better drugs.[35] Because of this fact, we became interested in rationalizing enthalpic favorability for the binding of SAHA to HDAC8 compared to that of its structural analogue (TSA) in light of the structural features of the HDAC8−TSA and −SAHA complexes. The structural data revealed that, unlike TSA, the carbonyl moiety of the anilino group of SAHA makes a specific hydrogen bond with Asp101 of HDAC8 (Figure 9),[29] which is similar to what has been observed for the binding of 3-(1-methyl-4-phenylacetyl-1*H*-2-pyrrolyl)-*N*-hydroxy-2-propenamide (APHA) to HDAC8.[36] Such a hydrogen bond could easily yield an enthalpic gain of 3−4 kcal/mol in the stabilization of SAHA (vis-à-vis TSA) to the active site pocket of HDAC8. However, we do observe that the activation enthalpy for the formation of the putative transition state from the free form of SAHA and HDAC8 is ∼2 kcal/mol higher than that for TSA, which could be attributed to an enthalpic penalty associated with the desolvation of polar moieties prior to the formation of the hydrogen bond described above.[37] A high enthalpic penalty for the attainment of the transition state for the HDAC8−SAHA interaction would further enhance the selectivity and specificity of the target−inhibitor interaction. The enthalpic gain obtained due to the formation of a specific hydrogen bond between SAHA and Asp101 is not translated into an increase in the binding affinity of the ligand. An entropic penalty of 2.0 kcal/mol is introduced presumably because of the reduction in the conformational flexibility of the protein and/or ligand upon hydrogen bonding. Unlike SAHA, the linker region of TSA does not form a hydrogen bond with Asp101, yielding a lower binding enthalpy.[29] Furthermore, the change in entropy (ΔS°) associated with the HDAC8−TSA encounter complex is entropically favored by 1.8 kcal/mol, which is translated into an enhanced binding affinity of the ligand. A larger entropic gain in the case of the binding of TSA to HDAC8 could largely be due to hydrophobic and nonpolar interactions. Hydrophobic interactions, in general, promote nonspecific interactions, and hence, it is not surprising to see that TSA would show considerable side effects in the cellular system because of its nonspecific binding to multiple off-target proteins. A cumulative account of these features clearly attests to the suitability of SAHA (over TSA) for the inhibition of HDAC8 not only at the enzymatic level but also presumably under the physiological condition. With this information, added to the fact that SAHA exhibits a better ADEM profile than TSA, it is not surprising that it has been chosen as a therapeutic agent for the treatment of T-cell lymphoma.

In conclusion, we have thoroughly elucidated the transient kinetics and the thermodynamics of the interaction of two structurally similar inhibitors (TSA and SAHA) with the recombinant form of human HDAC8. The experimental data provide the kinetic and thermodynamic rationale for SAHA being a more target-specific and -selective HDAC8 inhibitor than TSA; thus, SAHA can elicit a more selective inhibitory

dx.doi.org/10.1021/bi400740x | *Biochemistry* 2013, 52, 8139−8149

feature under the physiological condition. However, it should be clarified that our experimental data alone are not adequate to substantiate or refute the potential efficacy of SAHA versus TSA in a clinical setting.

AUTHOR INFORMATION

Corresponding Authors

*E-mail: raushan.singh@ndsu.edu. Phone: (701) 231-8483.
*E-mail: dk.srivastava@ndsu.edu. Phone: (701) 231-7831.

Funding

The research was supported by National Institutes of Health (NIH) Grants CA113746 and CA132034 to D.K.S. and S.M. and NIH COBRE Grant NCRR-P20-RR15566 to G.C.

Notes

The authors declare no competing financial interest.

ACKNOWLEDGMENTS

We acknowledge our research group members for valuable discussion on the contents of the manuscript.

REFERENCES

(1) Berger, S. L. (2002) Histone modifications in transcriptional regulation. *Curr. Opin. Genet. Dev. 12*, 142−148.

(2) Choudhary, C., Kumar, C., Gnad, F., Nielsen, M. L., Rehman, M., Walther, T. C., Olsen, J. V., and Mann, M. (2009) Lysine acetylation targets protein complexes and co-regulates major cellular functions. *Science 325*, 834−840.

(3) Reichert, N., Choukrallah, M.-A., and Matthias, P. (2012) Multiple roles of class I HDACs in proliferation, differentiation, and development. *Cell. Mol. Life Sci. 69*, 2173−2187.

(4) Gregoretti, I. V., Lee, Y.-M., and Goodson, H. V. (2004) Molecular evolution of the histone deacetylase family: Functional implications of phylogenetic analysis. *J. Mol. Biol. 338*, 17−31.

(5) Sauve, A. A., and Youn, D. Y. (2012) Sirtuins: NAD^+-dependent deacetylase mechanism and regulation. *Curr. Opin. Chem. Biol. 16*, 535−543.

(6) Gao, L., Cueto, M. A., Asselbergs, F., and Atadja, P. (2002) Cloning and functional characterization of HDAC11, a novel member of the human histone deacetylase family. *J. Biol. Chem. 277*, 25748−25755.

(7) Kazantsev, A. G., and Thompson, L. M. (2008) Therapeutic application of histone deacetylase inhibitors for central nervous system disorders. *Nat. Rev. Drug Discovery 7*, 854−868.

(8) McKinsey, T. A. (2012) Therapeutic potential for HDAC inhibitors in the heart. *Annu. Rev. Pharmacol. Toxicol. 52*, 303−319.

(9) Ropero, S., and Esteller, M. (2007) The role of histone deacetylases (HDACs) in human cancer. *Mol. Oncol. 1*, 19−25.

(10) Bolden, J. E., Peart, M. J., and Johnstone, R. W. (2006) Anticancer activities of histone deacetylase inhibitors. *Nat. Rev. Drug Discovery 5*, 769−784.

(11) Wagner, J. M., Hackanson, B., Lübbert, M., and Jung, M. (2010) Histone deacetylase (HDAC) inhibitors in recent clinical trials for cancer therapy. *Clin. Epigenet. 1*, 117−136.

(12) Subramanian, S., Bates, S. E., Wright, J. J., Espinoza-Delgado, I., and Piekarz, R. L. (2010) Clinical Toxicities of Histone Deacetylase Inhibitors. *Pharmaceuticals 3*, 275.

(13) Dokmanovic, M., Clarke, C., and Marks, P. A. (2007) Histone deacetylase inhibitors: Overview and perspectives. *Mol. Cancer Res. 5*, 981−989.

(14) Lipinski, C. A., Lombardo, F., Dominy, B. W., and Feeney, P. J. (1997) Experimental and computational approaches to estimate solubility and permeability in drug discovery and development settings. *Adv. Drug Delivery Rev. 23*, 3−25.

(15) Li, A. P. (2001) Screening for human ADME/Tox drug properties in drug discovery. *Drug Discovery Today 6*, 357−366.

(16) Kelly, W. K., O'Connor, O. A., Krug, L. M., Chiao, J. H., Heaney, M., Curley, T., MacGregore-Cortelli, B., Tong, W., Secrist, J. P., Schwartz, L., Richardson, S., Chu, E., Olgac, S., Marks, P. A., Scher, H., and Richon, V. M. (2005) Phase I study of an oral histone deacetylase inhibitor, suberoylanilide hydroxamic acid, in patients with advanced cancer. *J. Clin. Oncol. 23*, 3923−3931.

(17) Elaut, G., Laus, G., Alexandre, E., Richert, L., Bachellier, P., Tourwé, D., Rogiers, V., and Vanhaecke, T. (2007) A metabolic screening study of trichostatin A (TSA) and TSA-like histone deacetylase inhibitors in rat and human primary hepatocyte cultures. *J. Pharmacol. Exp. Ther. 321*, 400−408.

(18) Veber, D. F., Johnson, S. R., Cheng, H.-Y., Smith, B. R., Ward, K. W., and Kopple, K. D. (2002) Molecular Properties That Influence the Oral Bioavailability of Drug Candidates. *J. Med. Chem. 45*, 2615−2623.

(19) Navia, M. A., and Chaturvedi, P. R. (1996) Design principles for orally bioavailable drugs. *Drug Discovery Today 1*, 179−189.

(20) Lu, H., and Tonge, P. J. (2010) Drug−target residence time: Critical information for lead optimization. *Curr. Opin. Chem. Biol. 14*, 467−474.

(21) Borea, P. A., Dalpiaz, A., Varani, K., Gilli, P., and Gilli, G. (2000) Can thermodynamic measurements of receptor binding yield information on drug affinity and efficacy? *Biochem. Pharmacol. 60*, 1549−1556.

(22) Markgren, P.-O., Schaal, W., Hämäläinen, M., Karlén, A., Hallberg, A., Samuelsson, B., and Danielson, U. H. (2002) Relationships between structure and interaction kinetics for HIV-1 protease inhibitors. *J. Med. Chem. 45*, 5430−5439.

(23) Tummino, P. J., and Copeland, R. A. (2008) Residence time of receptor-ligand complexes and its effect on biological function. *Biochemistry 47*, 5481−5492.

(24) Lyons, D. S., Lieberman, S. A., Hampl, J., Boniface, J. J., Chien, Y., Berg, L. J., and Davis, M. M. (1996) A TCR binds to antagonist ligands with lower affinities and faster dissociation rates than to agonists. *Immunity 5*, 53−61.

(25) Freire, E. (2008) Do enthalpy and entropy distinguish first in class from best in class? *Drug Discovery Today 13*, 869−874.

(26) Ladbury, J. E., Klebe, G., and Freire, E. (2010) Adding calorimetric data to decision making in lead discovery: A hot tip. *Nat. Rev. Drug Discovery 9*, 23−27.

(27) Singh, R. K., Mandal, T., Balasubramanian, N., Cook, G., and Srivastava, D. K. (2011) Coumarin-suberoylanilide hydroxamic acid as a fluorescent probe for determining binding affinities and off-rates of histone deacetylase inhibitors. *Anal. Biochem. 408*, 309−315.

(28) Wiseman, T., Williston, S., Brandts, J. F., and Lin, L. N. (1989) Rapid measurement of binding constants and heats of binding using a new titration calorimeter. *Anal. Biochem. 179*, 131−137.

(29) Somoza, J. R., Skene, R. J., Katz, B. A., Mol, C., Ho, J. D., Jennings, A. J., Luong, C., Arvai, A., Buggy, J. J., Chi, E., Tang, J., Sang, B.-C., Verner, E., Wynands, R., Leahy, E. M., Dougan, D. R., Snell, G., Navre, M., Knuth, M. W., Swanson, R. V., McRee, D. E., and Tari, L. W. (2004) Structural snapshots of human HDAC8 provide insights into the class I histone deacetylases. *Structure 1993* (12), 1325−1334.

(30) Török, K., and Trentham, D. R. (1994) Mechanism of 2-chloro-(ε-amino-Lys75)-[6-[4-(N,N-diethylamino)phenyl]-1,3,5-triazin-4-yl]-calmodulin interactions with smooth muscle myosin light chain kinase and derived peptides. *Biochemistry 33*, 12807−12820.

(31) Dierynck, I., Wit, M. D., Gustin, E., Keuleers, I., Vandersmissen, J., Hallenberger, S., and Hertogs, K. (2007) Binding Kinetics of Darunavir to Human Immunodeficiency Virus Type 1 Protease Explain the Potent Antiviral Activity and High Genetic Barrier. *J. Virol. 81*, 13845−13851.

(32) Marks, P. A., and Breslow, R. (2007) Dimethyl sulfoxide to vorinostat: Development of this histone deacetylase inhibitor as an anticancer drug. *Nat. Biotechnol. 25*, 84−90.

(33) Naghibi, H., Tamura, A., and Sturtevant, J. M. (1995) Significant discrepancies between van't Hoff and calorimetric enthalpies. *Proc. Natl. Acad. Sci. U.S.A. 92*, 5597−5599.

(34) Leavitt, S., and Freire, E. (2001) Direct measurement of protein binding energetics by isothermal titration calorimetry. *Curr. Opin. Struct. Biol. 11*, 560−566.
(35) Kawasaki, Y., and Freire, E. (2011) Finding a better path to drug selectivity. *Drug Discovery Today 16*, 985−990.
(36) Dowling, D. P., Gantt, S. L., Gattis, S. G., Fierke, C. A., and Christianson, D. W. (2008) Structural Studies of Human Histone Deacetylase 8 and Its Site-Specific Variants Complexed with Substrate and Inhibitor. *Biochemistry 47*, 13554−13563.
(37) Cabani, S., Gianni, P., Mollica, V., and Lepori, L. (1981) Group contributions to the thermodynamic properties of non-ionic organic solutes in dilute aqueous solution. *J. Solution Chem. 10*, 563−595.